

# Validation of CFD Simulation for Ship Roll Damping using one Pure Car Carrier and one Standard Model

Min Gu, *China Ship Scientific Research Center, Wuxi, China*, [gumin702@163.com](mailto:gumin702@163.com)

Shuxia Bu, *China Ship Scientific Research Center, Wuxi, China*, [bushuxia8@163.com](mailto:bushuxia8@163.com)

Gengyao Qiu, *China Ship Scientific Research Center, Wuxi, China*, [xiaogeng502@163.com](mailto:xiaogeng502@163.com)

Ke Zeng, *China Ship Scientific Research Center, Wuxi, China*, [398638829@qq.com](mailto:398638829@qq.com)

Chengsheng Wu, *China Ship Scientific Research Center, Wuxi, China*, [cswu@163.com](mailto:cswu@163.com)

Jiang Lu, *China Ship Scientific Research Center, Wuxi, China*, [lujiang1980@aliyun.com](mailto:lujiang1980@aliyun.com)

## ABSTRACT

Ship roll damping is a key factor for predicting large amplitude roll motions, such as parametric roll and stability under dead ship condition. In this paper, the free roll motions of one pure car carrier and one international standard model ship 2792 for dead ship are simulated based on the unsteady RANS equations in calm water by two types of mesh, the sliding mesh and the overset mesh. The free roll decay curves of numerical simulations are compared with experimental results, and the roll damping coefficients are also compared with that from Ikeda's simplified formula. The calculated free decay curves agree quite well with the free decay curves from the experiments, and the errors of roll damping coefficient calculated by CFD are smaller than that from Ikeda's simplified formula, which validate that the unsteady RANS equations can be used to predict roll damping.

**Keywords:** *Roll damping, RANS, free rolling, commercial CFD codes*

## 1. INTRODUCTION

The large roll motions such as parametric roll and dead ship stability are one of critical risks for the safety when the ship sails in the seas, and the roll damping is essential to accurately predict these large roll motions. However, the accurate prediction of ship roll damping is very difficult, except for high cost experiments. Therefore, a numerical method to predict the large roll damping with high accuracy is desirable.

In general, most of the calculation methods are based on the potential theory, and the most common method is Ikeda's method (Ikeda, Y., 1977, 1978, 1979, 2000, 2004). These formulas can be used quite well for the conventional ships, but the prediction results are sometimes conservative or underestimated for unconventional ships (Japan, 2011a; Japan, 2011b; Sweden, 2011). This is because the large roll damping is strongly nonlinear, which has relationships with fluid viscosity and flow characteristics, such as the flow separation and vortex shedding. So the experience or semi-experience formulas can't take the full

consideration of different characteristics for different objects. Currently, the vulnerability criteria for parametric roll and dead ship stability are under development by International Maritime Organization (IMO) at second generation intact stability criteria, in which the roll damping coefficients were proposed using Ikeda's simplified method. Most of the calculated results of traditional ships by Ikeda's simplified method can fit experimental data quite well at the same order magnitude. However, if the size is outside the application range of Ikeda's method, or for the large amplitude motions in some phenomena, the accuracy will be low, which limit the application scope of Ikeda's method.

Except for Ikeda's simplified method, the Correspondence Group on Intact Stability regarding second generation intact stability criteria also proposed that the roll damping could be calculated by roll decay/forced roll test or CFD simulation (United States & Japan, 2014). Although the model tests can predict roll damping very well, but it is costly and time-consuming and most of experimental data are limited to a certain frequency

range and particular geometry, which is impossible for the large-scale expansion of the application (Bass & Haddara, 1988; Blok & Aalbers, 1991).

For the accurate calculation of roll damping, the influence of viscosity must be considered. The CFD numerical simulation can consider different objects and its characteristic, which can also reduce the cost. With the development of CFD technology, the turbulent models have been improved, such as RANS equation, discrete vortex method. In addition, the fine structure of the flow field can also be analyzed by CFD, so CFD could be widely used to predict roll damping. Forced roll method and free roll decay method are two main methods for the calculation of the roll damping.

In our previous studies (Min Gu, et al, 2015), the forced roll motions of one 2D ship section based on the methods of orthogonal design and variance analysis were carried out, in which different calculation parameters for the roll damping are analyzed, and the free motions of one 3D containership were also carried out.

The aim of this paper is to study the feasibility of CFD for the prediction of roll damping. The roll damping of one pure car carrier and ship 2792 which is provided by an IMO's intersessional corresponding group as one of standard ships for developing the second generation intact stability criteria are simulated based on the unsteady RANS equations in calm water, and two methods are used during numerical simulations, one is sliding interface method and another is dynamic overset grid method.

In the sliding interface technique, two cell zones are used, and they are contacted by a "mesh interface". The inner zone which is close to the bodies is moving with bodies, and the outer zone translates with bodies, which leads to the relative rotation between the outer zone and the inner zone. Overset meshes, also known as overlapping meshes, are used to discretize a computational domain with several different meshes that overlap each other in an arbitrary manner. Overset mesh has a background region enclosing the entire solution domain and one or more smaller regions containing the bodies within the domain. Both methods are most useful in problems dealing with moving bodies.

In this paper, the free roll decay curves as well as the roll damping coefficients calculated by both methods are compared with experimental results. Considering that the Ikeda's simplified method is recommended for the evaluation of roll damping coefficient in the latest drafts for parametric roll at second generation intact stability (Correspondence Group on Intact Stability, 2015), the results of roll damping coefficients are also compared with that from Ikeda's simplified formula.

## 2. SHIP GEOMETRY

The pure car carrier and the international standard model ship 2792 for dead ship stability with scale of 65.0 are adopted for the CFD computations. Main particulars of the pure car carrier and the standard model 2792 are given in Table 1 and Table 2. The body plans of the ship 2792 are shown in Fig.1, and the hull geometries of two models are shown in Fig.2 and Fig.3, respectively.

**Table 1: Principal particulars of the pure car carrier.**

Items	Model
Length: $L_{pp}$	3.5m
Mean draught: $T$	0.145m
Breadth: $B$	0.521 m
Depth: $D$	0.445m
$GM$	0.064 m
Displ.: $W$	169.23kg

**Table 2: Principal particulars of ship 2792.**

Items	Ship	Model
Length: $L_{pp}$	205.7m	3.165m
Mean draught: $T$	6.6m	0.102m
Breadth: $B$	32.0m	0.492m
Depth: $D$	20.2m	0.311m
$GM$	1.989m	0.0306m
Displ.: $W$	23986ton	87.34kg

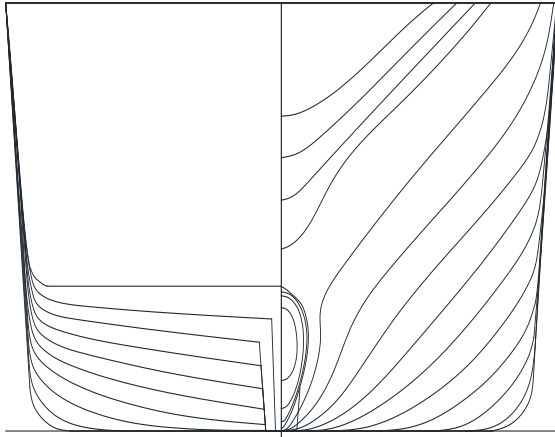


Figure 1: Lines of ship 2792.

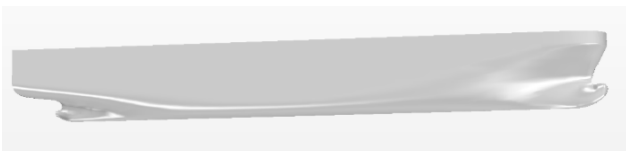


Figure 2: Hull geometry of the pure car carrier.



Figure 3: Hull geometry of ship 2792.

### 3. EXPERIMENTAL

Typical models used to study roll decay are usually with bilge keels which take account of the contribution of bilge keels to roll damping. However, for simply and basically, models without bilge keels in calm water are used in this paper. The free roll decay experiments for the pure car carrier are performed at the seakeeping basin (length: 69m, breadth: 46m, height: 4m) of CSSRC (China Ship Scientific Research Center), as shown in Fig.4, and the free roll decay experiments for ship 2792 are carried out at the towing tank of Wuhan University of Technology, as shown in Fig.5. The roll decay curves are measured by a MEMS (Micro Electro-Mechanical System)-based gyroscope placed on the ship model, and the initial roll angles are 10°, 20° and 25°, respectively.



Figure 4: Free roll decay tests of the pure car carrier.

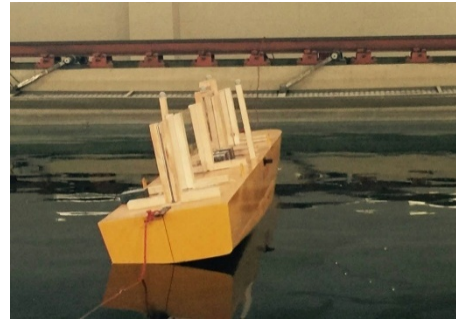


Figure 5: Free roll decay tests of ship 2792.

### 4. COMPUTATION METHOD

#### Mathematical model and numerical method

All computations are performed by solving unsteady RANS equations. RNG k-ε two-equation model is employed for the enclosure of the governing equations. The VOF method is adopted for the treatment of nonlinear free surface. The pressure-correction algorithm of SIMPLE type is used for the pressure-velocity coupling. Two methods are used during simulations, one is the sliding mesh, and another is the overset mesh. The enhanced wall function is adopted based on the previous studies (Min Gu, et al, 2015).

In simulations, the modes of roll, sway and heave are free and other modes are constrained. The solution domains are shown in Figs.6 and 7, and the types of body meshes are shown in Fig.8 and Fig.9, respectively. The boundary of the computational domain is composed of inlet boundary, outlet boundary, wall boundary (hull surface), and outlet boundary.

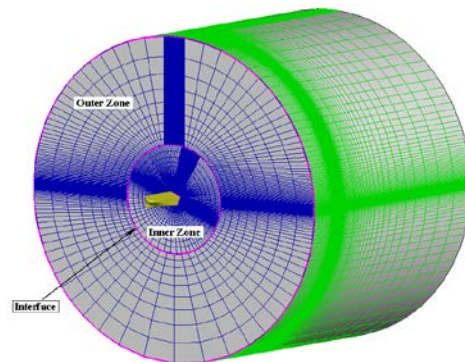


Figure 6: Computational domains and meshes with the sliding mesh method.

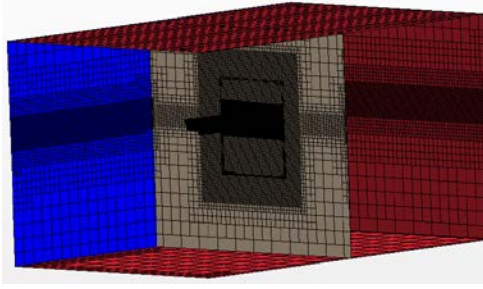


Figure 7: Computational domains and meshes with the overset mesh method.

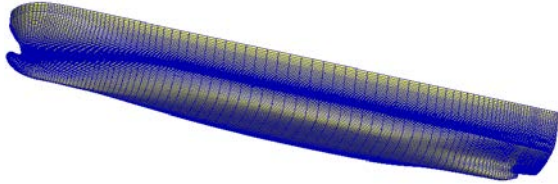


Figure 8: Hull meshes of the pure car carrier.



Figure 9: Hull meshes of ship 2792.

### Analysis methods

According to the latest drafts for the vulnerability criteria of parametric roll (Correspondence Group on Intact Stability, 2015), if we introduce the equivalent linear damping coefficient  $B_{44}(\phi_a)$ , the roll motion in calm water can be modelled as:

$$(I_{xx} + J_{xx})\ddot{\phi} + B_{44}(\phi_a)\dot{\phi} + WGM\phi = 0 \quad (1)$$

Where,  $I_{xx} + J_{xx}$ : virtual moment of inertia in roll,  $W$ : ship weight,  $GM$ : initial metacentric height. Then:

$$\ddot{\phi} + 2\alpha\dot{\phi} + \omega_\phi^2\phi = 0 \quad (2)$$

$$\text{Where, } 2\alpha = \frac{B_{44}(\phi_a)}{I_{xx} + J_{xx}}, \omega_\phi = \sqrt{\frac{WGM}{I_{xx} + J_{xx}}}$$

In Ikeda's simplified formula,  $B_{44}$  is normalized as follow:

$$\hat{B}_{44} = \frac{B_{44}}{\rho \nabla B^2} \sqrt{\frac{B}{2g}} \quad (3)$$

Where,  $B$ : ship breadth,  $\nabla$ : ship displacement volume and  $\rho$ : water density.

In order to compare the results of roll damping coefficients between CFD and Ikeda's simplified formula, the extinction curve should be expressed

as the linear formula (4), which is the essential component of roll damping.

$$\phi = A\phi_m \quad (4)$$

Where,  $\Delta\phi$ :decrement of roll decay curve and  $\phi_m$ :mean swing angle of roll decay curve.

The linear fitting coefficient  $A$  can also be calculated as formula (5), for the conservation of energy.

$$A = \frac{T_\phi}{4(I_{xx} + J_{xx})} B_{44}(\phi_a) \quad (5)$$

Thus,

$$2\alpha = \frac{4A}{T_\phi} \quad (6)$$

The results of  $2\alpha$  are compared for different methods, which can analyze the combined error of roll amplitude and roll period. The natural roll periods measured in model tests are used in the Ikeda's simplified formula, taking into consideration that only the equivalent roll damping coefficient can be calculated by Ikeda's simplified formula.

## 5. THE CALCULATION RESULTS AND ANALYSIS

### The grid analysis

Based on our previous studies, a simple grid analysis is given out before the numerical simulation for the dynamic overset grid method.

Taking the pure car carrier as an example, the profile of the computational domain is shown in Fig.10. The computational domain is separated into two main regions, background region and overset region, and each region is further divided into several small zones. The meshes in overlap region are refined to guarantee the data exchange between overset region and background region. The waterline plane region is also refined to capture the free surface.

Generally, the size for the background region and the overset region should be large enough to simulate actual situation. However, the size of the overset region should be as small as possible to reduce computation cost in the actual simulations. In this paper, two different widths of overset region are analyzed, one is 4B(S1) and another is 5B(S2). This is because the width is the main influential size when simulating free roll motion in calm water.

The comparison results shown in Fig.11 show that the two curves are almost the same, which meaning that the width 4B is enough for the simulations.

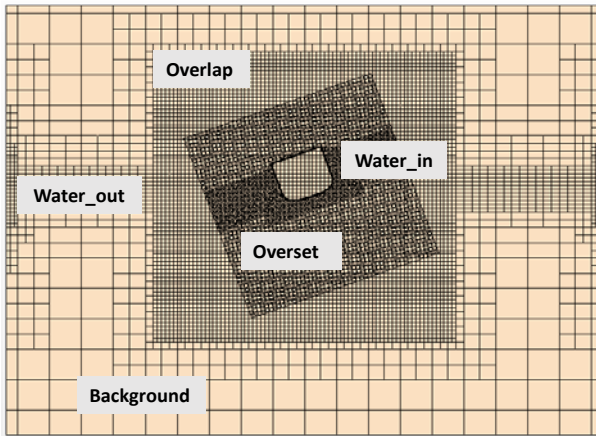


Figure 10: The profile of computational domain for the overset grid method.

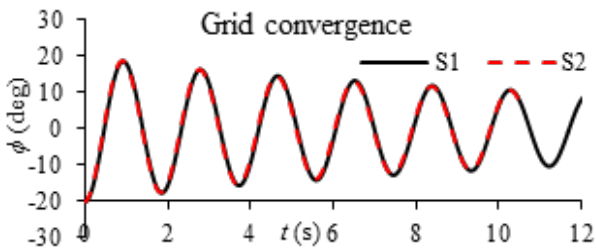


Figure 11: Comparisons between different widths of overset region.

Three cases for the grid convergence are also carried out to confirm grid density. In the first case shown as V1 in Fig.12, the base size for the background domain is equal to 0.08 and the base size for the overset domain is equal to 0.04. In the second case shown as V2, the base size is decreased to 0.07 for the background domain and 0.035 for the overset domain. In the third case shown as V3, the base size is kept for the background domain and the base size for the overset domain is decreased to 0.03. The results show that the base size in the first case is small enough for the numerical simulations.

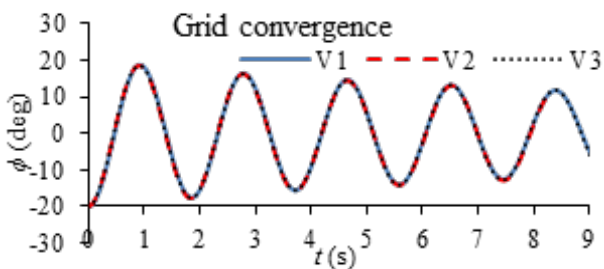


Figure 12: Comparisons between different base sizes.

### The results of pure car carrier

For the free roll decay motions of the pure car carrier, the comparisons between numerical simulation results and experimental results are presented from Fig.13 to Fig.18. The results of coefficient  $2\alpha$  in formula (2) and (6) calculated by different methods are compared in Table 3.

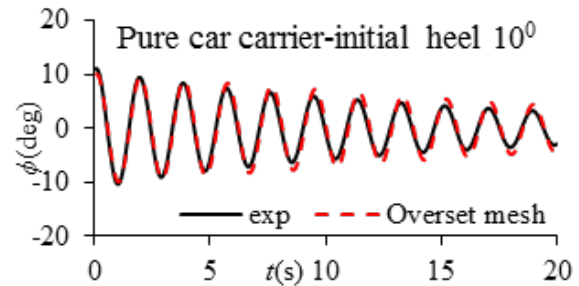


Figure 13: Free decay curves for the pure car carrier with initial heel 10°(exp, overset mesh).

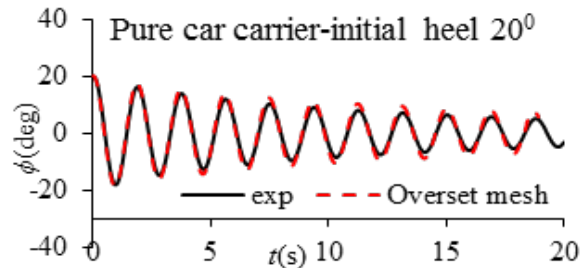


Figure 14: Free decay curves for the pure car carrier with initial heel 20°(exp, overset mesh).

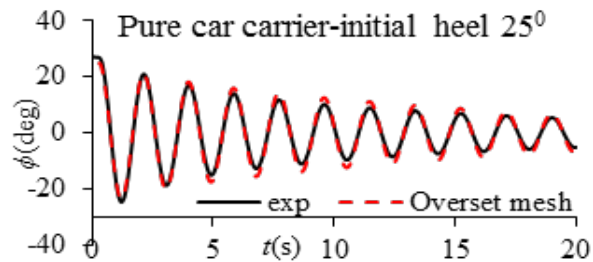


Figure 15: Free decay curves for the pure car carrier with initial heel 25° (exp, overset mesh).

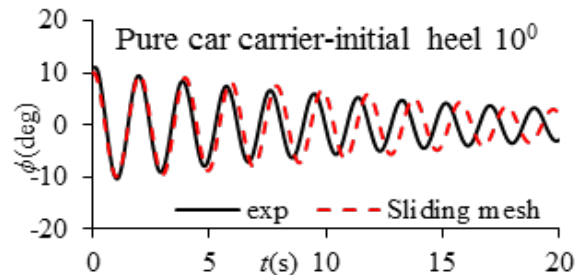


Figure 16: Free decay curves for the pure car carrier with initial heel 10°(exp, sliding mesh).

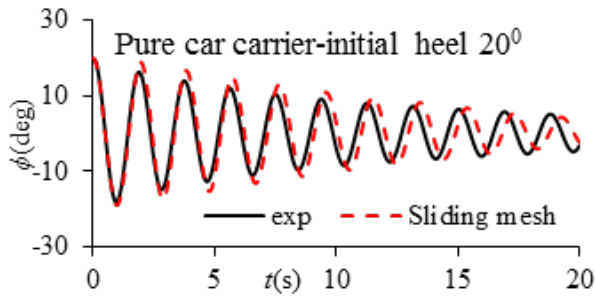


Figure 17: Free decay curves for the pure car carrier with initial heel 20° (exp, sliding mesh).

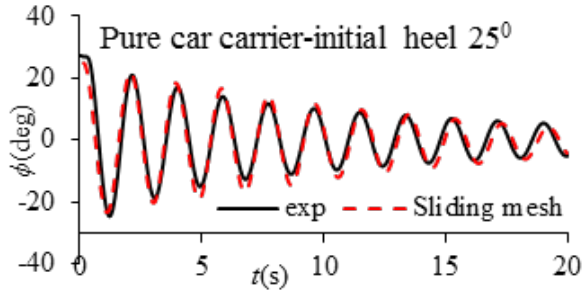


Figure 18: Free decay curves for the pure car carrier with initial heel 25° (exp, sliding mesh).

As can be seen from these figures, the roll periods calculated by the overset grid method agree better with the experimental data than that by the sliding mesh method, but the roll amplitudes calculated by the sliding mesh method are better than that by the overset grid method. Although the roll damping coefficients calculated by CFD are better than that in Ikeda's simplified formula, the errors of the pure car carrier are larger than the ship 2792 (Table 4), so the feasibility for different types of ship and different conditions should be further verified.

Table 3: Results of  $2\alpha$  calculated by different methods for the pure car carrier.

Initial heel	Exp	Overset mesh		Sliding mesh		Ikeda	
	Value	Value	Error	Value	Error	Value	Error
10°	0.0082	0.0050	39.02%	0.0060	26.83%	0.0046	43.90%
20°	0.0103	0.0082	20.39%	0.0089	13.59%	0.0072	30.10%
25°	0.0119	0.0092	22.69%	0.0100	15.97%	0.0085	28.57%

**The results of standard model 2792**

For the free roll decay motions of ship 2792, the initial roll angles 10°, 20° and 25° are simulated respectively by two methods, as shown from Fig.19 to Fig.24, and the results of coefficient  $2\alpha$  are shown in Table 4.

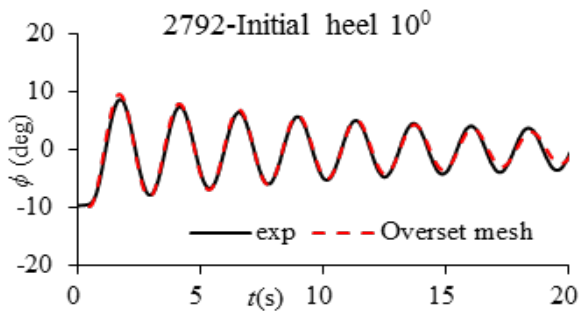


Figure 19: Free decay curves for ship 2792- initial heel 10° (exp, overset mesh).

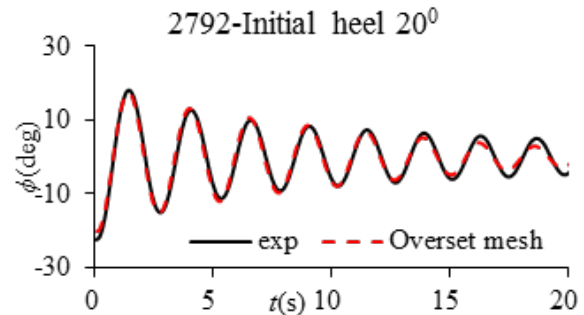


Figure 20: Free decay curves for ship 2792- initial heel 20° (exp, overset mesh).

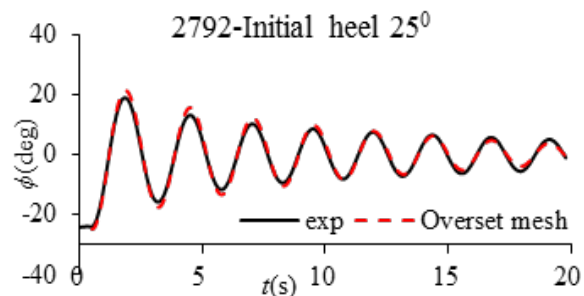


Figure 21: Free decay curves for ship 2792- initial heel 25° (exp, overset mesh).

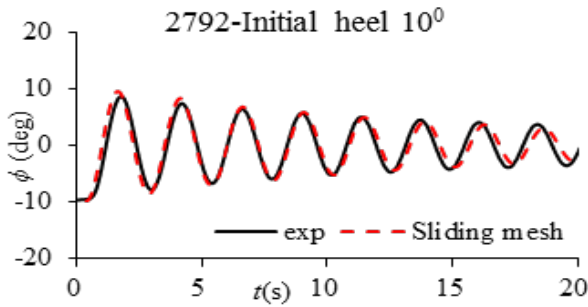


Figure 22: Free decay curves for ship 2792- initial heel 10° (exp, sliding mesh).

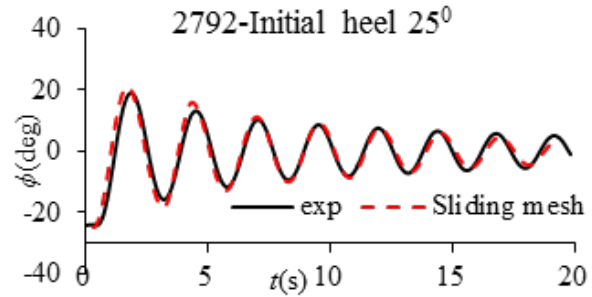


Figure 24: Free decay curves for ship 2792- initial heel 25° (exp, sliding mesh).

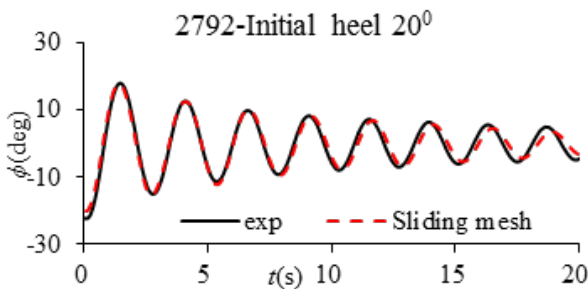


Figure 23: Free decay curves for ship 2792- initial heel 20° (exp, sliding mesh).

The curves show that the periods and amplitudes calculated by the overset grid method agree better with the experimental data than that by the sliding mesh method. The results of roll damping coefficient  $2\alpha$  also show that the accuracy of CFD is higher than Ikeda's simplified formula.

Table 4 Results of  $2\alpha$  calculated by different methods for ship 2792

Initial heel	Exp	Overset mesh		Sliding mesh		Ikeda	
	Value	Value	Error	Value	Error	Value	Error
10°	0.0076	0.0084	10.53%	0.0079	3.95%	0.0088	15.79%
20°	0.0122	0.0127	4.10%	0.0110	9.84%	0.0156	27.87%
25°	0.0157	0.0156	0.64%	0.0137	12.74%	0.0192	22.29%

## 6. CONCLUSIONS

As the comparisons for the free rolling motions of one standard model and one pure car carrier among two numerical simulation methods, Ikeda's simplified method and experiments, the following remarks are noted:

1) For the method of dynamic overset grid, the natural roll periods agree quite well with experimental results, but the roll amplitudes are slightly larger than experimental results. For the method of sliding interface grid, both the natural roll period and the roll amplitude are slightly larger than experimental results.

2) The roll damping coefficients calculated by CFD are better than that calculated by Ikeda's simplified formula, which indicate that CFD based on unsteady RANS equations has the ability to predict roll damping, at least for large roll amplitudes.

3) Based on our current studies, the following combination of calculation parameters are recommended when simulating free roll decay motion, unsteady RANS equations combined with RNG  $k-\epsilon$  / SST  $k-\omega$  two-equation turbulent model to solve flow field, VOF method to capture free surface, sliding interface technique or dynamic overset mesh technique to compute bodies motions, enhanced wall function to treat near-wall boundary layer.

In our simulations, neither of the two ships has bilge keels. However, the bilge keel damping contributes a large portion to the total damping (Bassler & Reed, 1999), so more works should be carried out in future to validate the feasibility of CFD for roll damping, and to improve the accuracy, especially for the unconventional ship with bilge keels.

## 7. ACKNOWLEDGEMENTS

This research is supported by Ministry of Industry and Information Technology of China (No. [2012] 533 , No. [2016] 26) and China researchfund (No.B2420132001). The authors sincerely thank the above organization

## 8. REFERENCES

- Blok, J.J., & Aalbers, A.B., 1991, "Roll Damping Due to Lift Effects on High Speed Monohulls", FAST'91, Vol. 2, pp. 1331-1349.
- Bassler C.C., Reed A.M., 2009, "An Analysis of the Bilge Keel Roll Damping Component Model", 10<sup>th</sup> STAB, St. Petersburg, Russia. pp:369-386.
- Min Gu, Jiang Lu, Shuxia Bu, Chengsheng Wu, Gengyao Qiu, 2015, "Numerical Simulation of the Ship Roll Damping", 12<sup>th</sup> STAB, Glasgow UK, pp:341-348.
- Ikeda, Y., Himeno, Y., & Tanaka, N., 1977a, "On Eddy Making Component of Roll Damping Force on Naked Hull", Journal of the society of Naval Architects of Japan. Vol. 162, pp. 59-69.
- Ikeda, Y., Komatsu, K., Himeno, Y., & Tanaka, N., 1977b, "On Roll Damping Force of Ship-Effect of Hull Surface Pressure Created by Bilge Keels", Journal of the society of Naval Architects of Japan, Vol. 165, pp. 31-40
- Ikeda, Y., Himeno, Y., & Tanaka, N., 1978, "Components of Roll Damping of Ship at Forward Speed", Journal of the society of Naval Architects of Japan, Vol. 143, pp. 113-125.
- Ikeda, Y., & Katayama, T., 2000, "Roll Damping Prediction Method for a High-Speed Planning Craft", Proceedings of the 7th International Conference of Ships and Ocean Vehicles (STAB'2000), Vol. 2, PP. 532-541.
- Ikeda, Y., 2004, "Prediction Methods of Roll Damping of Ships and Their Application to Determine Optimum Stabilization Devices", Marine Technology. Vol.41(2) , pp. 89-93.
- ISCG (the Correspondence Group on Intact Stability), 2015, "Draft Explanatory Notes on the Vulnerability of Ships to the Parametric Roll Stability Failure Mode", IMOSDC3/INF.10, Annex 17.
- Japan, 2011a, "Interim Verification and Validation Report on Simplified Roll Damping", IMO SLF 54/INF 12, Annex 7.
- Japan, 2011b, "Additional Validation Data on Simplified Roll Damping Estimation for Vulnerability Criteria on Parametric Rolling", IMO SLF 54/INF 12, Annex 11.
- Sweden, 2011, "Evaluation of Ikeda's simplified method for prediction of roll damping", IMO SLF 54/3/6.
- United States & Japan, 2014, "Draft Guidelines of Direct Stability Assessment Procedures as a Part of the Second Generation Intact Stability Criteria, IMO SDC1/INF.8, Annex 2.